Robotics Reports Volume 1.1, 2023 DOI: 10.1089/rorep.2023.0017 Accepted September 24, 2023



Open camera or QR reader and scan code to access this article and other resources online.



ORIGINAL ARTICLE

Open Access

A Novel Variable Impedance Actuator Utilizing Adjustable Viscoelastic Properties of Thermoresponsive *Polycaprolactone*

Trevor Exley, MS, Daniel Johnson, MS, and Amir Jafari, PhD*

Abstract

This article presents a design for a variable impedance actuator capable of changing stiffness and damping through the heating of a thermoplastic polymer, in an off-line manner. Typically, other actuators have additional mechanisms to regulate overall impedance, but the key component of this design uses *polycaprolactone*. This polymer exhibits temperature-dependent viscoelastic properties, so that at room temperature, it is rigid, and softens as temperature increases. Flexible heaters are embedded into the design for adjusting the output impedance. The variable impedance module has fixed elastic components in parallel with the variable elastic and damping components of the polymer. To show the effect of variable impedance, the motor was set to follow sinusoidal trajectories while the position of the output link was measured. As an indicator for change in the output impedance, the actuator exhibits a fivefold increase in overshoot due to a 40°C temperature increase. Although adjusting the output impedance of this device is not suitable for on-line implementation, the design is scalable and can be made compact through miniaturization of components.

Keywords: polycaprolactone; VIA; variable impedance actuator; thermoresponsive polymer

Introduction

As robotic platforms increasingly encounter unfamiliar environments, *physical* human–robot interactions (*p*HRIs) are becoming more commonplace. To ensure safety and improve their resilience, these robotic systems need to adjust their level of impedance. Impedance refers to the resistance to motion, which comprises stiffness, damping, and inertia. Variable impedance actuators (VIAs)² are a novel solution for creating compliant systems that can physically interact

with humans. These actuators are capable of modifying their impedance by changing their stiffness,^{3–5} damping ratio,^{6,7} or even their inertia⁸ when in contact with unknown environments. The purpose of this is to ensure the safety of humans interacting with robots while simultaneously improving performance criteria.³

The primary subset of VIAs are variable stiffness actuators (VSAs),⁹ which regulate only the stiffness component of the output link's impedance during physical interactions with external environments.

Advanced Robotic Manipulators (ARM) Lab, Department of Biomedical Engineering, University of North Texas, Denton, Texas, USA.

[©] Trevor Exley et al., 2023; Published by Mary Ann Liebert, Inc. This Open Access article is distributed under the terms of the Creative Commons License [CC-BY] (http://creativecommons.org/licenses/by/4.0), which permits unrestricted use, distribution, and reproduction in any medium, provided the original work is properly cited.



^{*}Address correspondence to: Amir Jafari, PhD, Advanced Robotic Manipulators (ARM) Lab, Department of Biomedical Engineering, University of North Texas, 3940 N Elm St, Denton, TX 76207, USA, Email: amir.jafari@unt.edu

Variable damper actuators^{7,10} and variable inertia actuators¹¹ are the other two subsets of VIAs, but they have garnered less attention in robotics research. The reason for this is that these designs lack energy-saving and releasing components compared with VSAs, resulting in less potential for reducing energy consumption in periodic motions.^{12–15} However, damping is necessary in applications wherein the system's overall energy must be kept below a certain threshold to ensure stability, such as knee joints in bipedal robots, which require the addition of damping to release energy.

VIAs should be able to control at least two degrees of freedom (*i.e.*, link's trajectory and link's impedance) and require at least two independent sources of generating mechanical power (*i.e.*, flow and effort)¹⁶ such as electric motors.^{17,18} If both damping and stiffness need to be controlled on top of the link trajectory, then three motors will be required.

In general, altering the impedance parameters of an actuator requires a dedicated mechanism that is incorporated into the actuator's design. However, incorporating such mechanisms results in bulky, heavy, and large actuators compared with traditional rigid or series elastic actuators (SEAs). The bulkiness is the most significant practical drawback of VIAs, which limits their suitability in many applications. The extra components that are added to the design increase the inertia of the actuator, thereby decreasing its safety criterion for human–robot interaction (HRI) applications. ^{21–23}

Currently, SEAs are preferred over VIAs, even in applications that require impedance adjustments, such as bipedal locomotion^{24–27} and manipulation.^{28–30} At the miniature scale, low-power actuators that use heating in the form of shape-memory alloys have been investigated.³¹ Outside of HRI applications, variable impedance is necessary for automation, task execution, and traversal of unknown environments.^{32,33} In this article, we present a novel thermal-based VIA, as shown in Figure 1.

As with other series classes of VIAs, ¹⁹ a DC motor is typically used to command the position of the output link of the actuator. However, our VIA design is unique in that the actuator's impedance is adjusted by controlling the temperature of a thermoplastic polymer, polycaprolactone (PCL), instead of a mechanical mechanism. PCL is a thermoplastic polymer that falls under the category of polymers that exhibit changes in viscoelasticity as they transition from cold (rigid) to hot (soft).³⁴ PCL's reversible ability to change stiff-

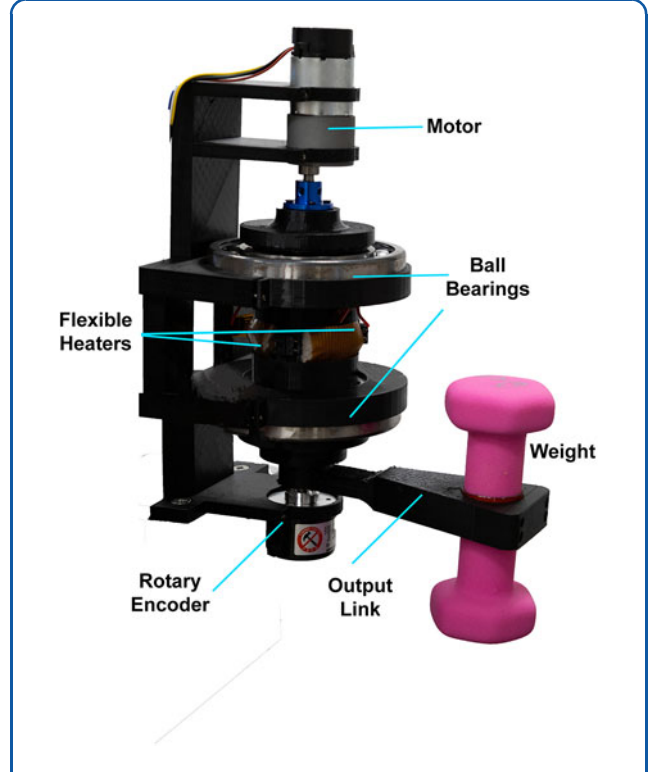


FIG. 1. Thermoactive VIA prototype constructed with 3D-printed PETG components with integrated flexible polyimide heaters. A weight of 0.91 kg is attached at the output link. PETG, polyethylene terephthalate glycol.

ness at human-safe temperatures makes it a promising material for *p*HRI applications.

To control the temperature, flexible polyimide heaters are embedded in our design.³⁵ Since a simple mechanism is sufficient for adjusting the impedance, our design enables compact and lightweight variable impedance actuation technology. The focus of this study is to characterize the model for impedance adjustment and evaluate the tracking capabilities of the actuator at different configurations.

The organization of this article is as follows: in Mechanical Design and Components of the Proposed PCL-Based VIA section, the key components of the thermal-based VIA will be introduced. Material characterization of the PCL will be discussed in Modeling the Viscoelasticity of the Proposed VIA section. Experimental Results section uses data from a trajectory tracking experiment to regulate impedance, and finally discussion and conclusion are presented in Discussion and Conclusion section.

Mechanical Design and Components of the Proposed PCL-Based VIA

The VIA that we have designed comprises a DC motor and gearbox that are connected in series with a thermoactive variable impedance module. The module includes embedded compression springs that provide a fixed level of compliance, and a PCL polymer that allows for a tunable damping ratio. The output of the thermoactive module is then connected to the actuator's link. In this section, we present the mechanical design of our proposed VIA, along with an explanation of how we fabricated a prototype.

Mechanical design

The thermoactive module in our proposed design has the following essential components as shown in Figure 2a–c: an outer ring attached to a fixed base that holds the PCL inside, and three radially mounted flexible polyimide heaters. The heaters are located in slots that have access to the outside environment. The reason for this mounting is so that the generated

heat can be taken out of the system, otherwise it could damage electronic components and potentially lead to their failure. A prototype of the proposed VIA is shown in Figure 1.

To couple the variable impedance module to the motor, a spiked wheel is placed inside the outer ring and is attached to the output link, whereas the housing is attached firmly to the motor shaft. The spikes on the wheel are in contact with the PCL material that is also located inside the outer ring of the housing. As the output link moves, the spiked wheel rotates within the housing, pushing the PCL through its spikes. Each spike is connected to the housing *via* compression springs. When the wheel rotates within the outer ring due to the motion of the output link, the compression springs become deformed, causing the output link to behave in a compliant manner.

By placing the springs between the output link and the fixed end, our design acts like a SEA. However, the addition of PCL in the housing allows adjustment of the temperature to change the overall

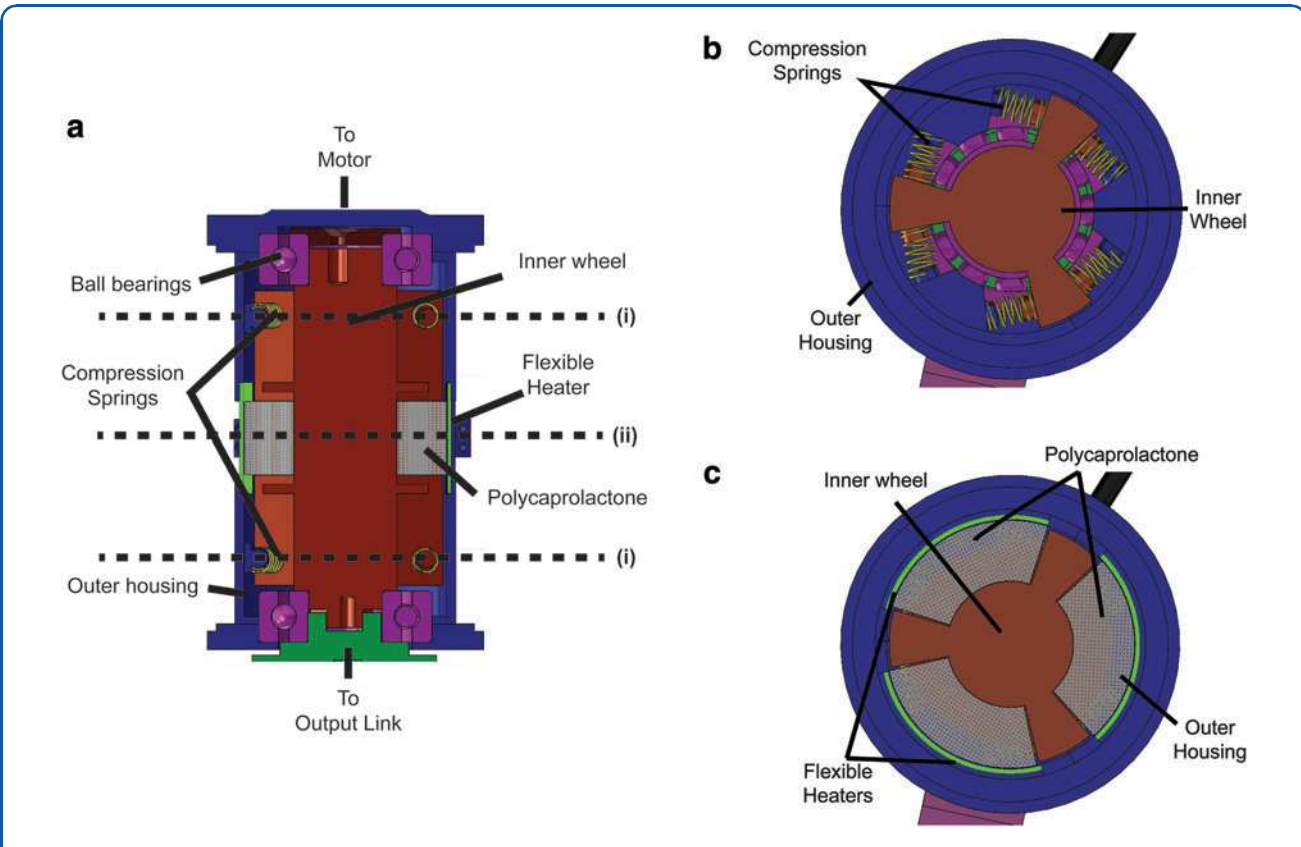


FIG. 2. CAD design of thermoactive VIA. **(a)** Side view of VIA body, **(b)** top view of VIA body at (i), **(c)** top view of VIA body at (ii). PCL, polycaprolactone; VIA, variable impedance actuator.

impedance of the system, utilizing the viscoelastic properties of PCL to create variable impedance behavior.

Next, the essential components of our physical prototype such as the PCL will be discussed in detail.

Components of the VIA prototype

All housing components, the output link, and fixed base of the VIA prototype outlined in Figure 2a were 3D printed. Polyethylene terephthalate glycol (PETG) was chosen for the filament as it has better shock resistance than traditional PLA and can withstand the higher range of temperatures from the heaters without melting or warping.

PCL is a biodegradable polyester that is known for its viscoelastic properties. It has a low melting point of around 60°C and a glass transition temperature of about -60°C. It is made by using a process called ring-opening polymerization, which is a type of chain-growth polymerization that involves the initiation of a polymer chain to attack cyclic monomers to form a longer polymer. This method is commonly used to make biopolymers. Owing to its viscoelasticity, PCL can change its degree of stiffness as temperatures move from cold (rigid) to hot (soft), making it a versatile material for various applications. The structure of PCL is shown in Figure 3a. This chain resulted from ring-opening polymerization in PCL makes it a thermoplastic polymer.

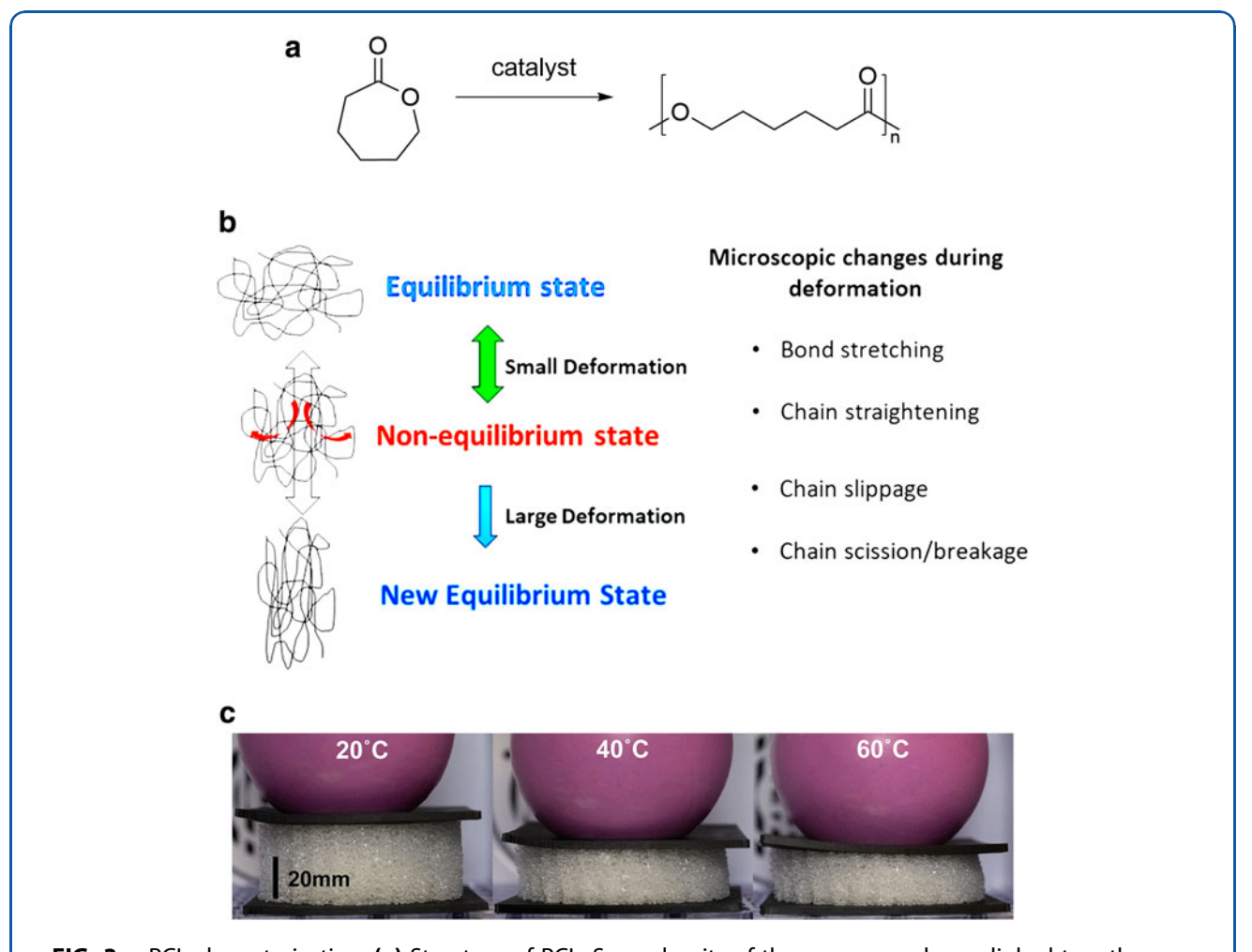


FIG. 3. PCL characterization. **(a)** Structure of PCL. Several units of the monomer shown linked together in a chain to form the polymer. **(b)** Recoverable and permanent deformations of a polymer due to the external forces. **(c)** Compression of PCL sponge with 4.5 kg of added weight at (L to R) 20°C, 40°C, and 60°C.⁴⁴

As a polymer, PCL exhibits viscoelastic behaviors as it undergoes both recoverable and permanent deformations depending on the levels of applied forces. Polymeric chains can have motions at different timescales: from atomic vibrations to full chain diffusion. Diffusion of large segments of chains occurs at a much slower speed than diffusion of small segments. Owing to this property, polymeric materials have time-dependent deformations.

In the absence of an external force, the morphology of the polymer chain is determined by the internal forces, such as chemical bond, intermolecular interactions, segmental mobility, entanglements, and crystals.³⁸ At this morphology, the internal forces continuously interact with each other to form the lowest possible state. This state is a highly disordered form of chains called the equilibrium state. When an external force is applied, it leads to the alignment of some polymer chains in the force direction. However, other polymer chains try to pull the affected chains back to the original position through the entanglement points.³⁹

At small deformations, bond and chain strengthening⁴⁰ can take place. Both deformations act like strengthening a spring, so the polymer will return to its original shape once the force is removed (Fig. 3a). In contrast, if the polymer chain is deformed further or the load is applied for a long time, then chain breakage and slippage^{41,42} can occur. Both phenomena would result in a permanent change in the polymer morphology. As a result, when the force is removed, the chain will not be able to return to its original shape and it will retain a new equilibrium state.

PCL is a plastic polymer that becomes moldable at high temperatures and solidifies upon cooling. It is a thermoplastic with high molecular weight, and its polymer chains associate through intermolecular forces, which weaken at high temperatures. As a result, PCL becomes a viscous liquid that can be reshaped and is commonly used in polymer processing techniques. Its degree of stiffness changes as temperature increases, becoming softer as it gets hot and rigid as it cools.

To determine the impedance variation of PCL as a function of temperature, some static tests have been done⁴⁴ (*i.e.*, evaluating stiffness component of the impedance) on a sponge made of PCL. In these experiments (shown in Fig. 3c), a known weight (4.5 kg) was placed on the sponge while the temperature changed from 20°C to 60°C. The vertical deflection of the sponge was then measured and then normalized

with its original thickness to determine the strain. Similarly, the weight was divided by the area of the sponge to calculate the stress.

Modeling Viscoelasticity of the Proposed VIA

To fully characterize the impedance of our design, the viscoelastic properties of PCL, that is, its storage E_1 , G_1 and loss E_2 , G_2 moduli (tensile and shear), as functions of temperature T, must be considered. Figure 4 shows both tensile moduli decreasing dramatically when the temperature exceeds 30°C. Below this threshold temperature, $E_2 \leq E_1$ and $G_2 \leq G_1$ imply that the elastic behavior of the material is more dominant than its viscous property. When the temperature is higher than 45°C, PCL becomes very soft and will be a more viscous material rather than an elastic material as $G_2 \leq G_1$.

In our proposed design, the compression springs, mounted radially around the wheel, can be modeled as fixed springs in parallel with the PCL modeled as a variable spring and dashpot. The two primary methodologies for modeling viscoelastic materials are Maxwell⁴⁶ or Kelvin-Voigt⁴⁷ models. Both models use springs to depict a pure elastic element and a dashpot to represent a pure viscous element.

These models differ in how they apply stress and strain to these elements. In the Maxwell model, both the spring and dashpot experience the same stress, whereas each element has an independent strain. In contrast, in the Kelvin-Voigt model, both the spring

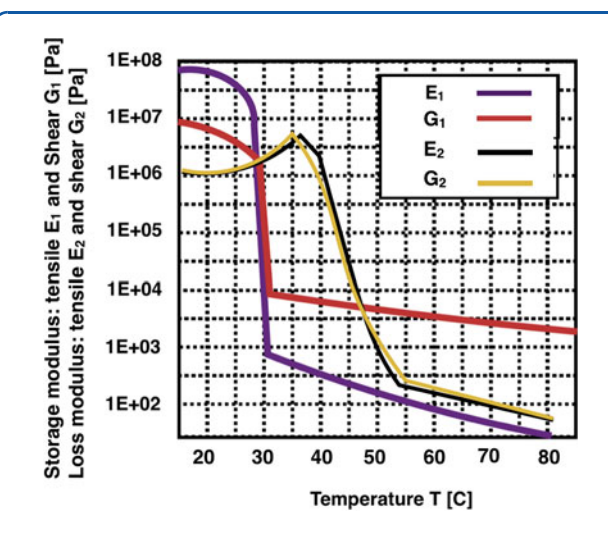


FIG. 4. Storage and loss (tensile and shear) moduli of PCL at different temperatures (adapted from Mosleh et al.).⁴⁵

and the dashpot are subjected to the same strain, but each element has independent stress. Although the Maxwell model is better at predicting the recovery phase (after releasing the external load), the Kelvin–Voigt model can more accurately represent the strain rate–time dependency that is fundamental in viscoelastic behavior, such as the creep phenomenon.⁴⁸

When modeling a viscoelastic material that exhibits pre-dominant elasticity, the Kelvin–Voigt model is typically preferred for describing the creep behavior of the material, due to its practicality and wide application in the engineering field.⁴⁹

In our design, we present the PCL as a Kelvin–Voigt model, since the compression springs will be modeled as a spring in parallel with PCL, which will have higher stiffness than that of the spring in the PCL model at higher temperatures.

The schematic of the VIA model is presented in Figure 5. The output link is attached to the variable impedance module that is connected to the DC motor. The variable impedance unit is composed of a damper to represent viscosity of PCL b_{PCL} , a spring to represent elasticity of PCL k_{PCL} , and a spring for the compression springs with constant stiffness K_s . The output link's position is shown by θ_L , whereas the position of the motor end is shown by θ_M .

Similarly the torque at the output of the motor end is T_M and T_L is the output torque available at the output link of the actuator. The flexible heater generates heat to increase the temperature of the PCL. Changing the temperature alters the tensile and shear storage and loss moduli of PCL (E_1 , G_1 , E_2 , G_2), thus changing overall elasticity and viscosity. (k_{PCL} and b_{PCL}).

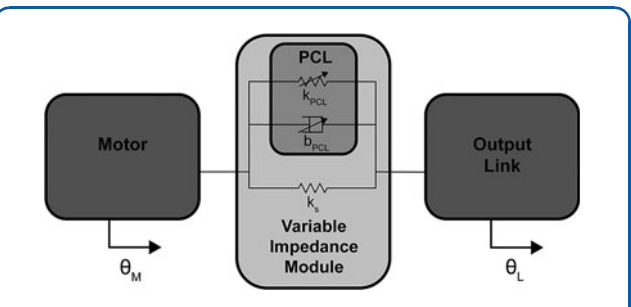


FIG. 5. Schematic model of the proposed variable impedance module, located in series between the motor and the output link and powered through the flexible heaters.

The equation of motion for the output link as a result of the output torque, and while the output of the torque is 0 (*i.e.*, $T_L = 0$) is as follows:

$$T_M = b_{PCL} \left(\dot{\theta}_L - \dot{\theta}_M \right) + (k_{PCL} + k_s) (\theta_L - \theta_M) + I_L \ddot{\theta}_L, \quad (1)$$

where I_L is the link's inertia and T_M is the torque available at the output of the motor that already has the motor/gearbox inertia and damping components in it. In terms of stress–strain, the Kelvin–Voigt model leads to the following equation:

$$\sigma(t) = E_1 \epsilon(t) + \eta(G_2) \frac{d\epsilon(t)}{dt}, \qquad (2)$$

where η is the viscosity of PCL that is related to the loss modulus as $\eta = \frac{G_2}{\omega}$, where ω is the frequency of the loading signal.

Experimental Results

To examine the capability of our proposed VIA in regulating the overall impedance of the output link, the motor was set to follow trajectories as $\theta_M(t) = A sin(\omega t)$, where A is the amplitude of the signal in degree, and ω is the angular frequency of the signal, as mentioned before. The actual position of the output link was then measured using the dedicated encoder as shown in Figure 1. This experiment was done at different temperatures and frequencies.

The PCL temperature was set at different levels from room temperature (22°C) to 60°C using the flexible heaters. The goal was to show how the temperature can affect the time-dependent impedance of PCL as the creep and stress relaxation behaviors, that is, the response of the output link to the driving motor signal was plotted.

System identification

For the purpose of system identification, a sinusoidal trajectory with varying frequency was applied to the motor shaft. Simultaneously, the trajectories of both the output link and the motor shaft were tracked at each frequency using dedicated encoders. It is important to note that the deviation between the commanded trajectory for the motor shaft and the actual trajectory of the output link is the result of the system compliance. This compliance is a combination of stiffness and damping of the output link both affected by the temperature of the *polycaprolactone* polymer. The model was then validated by comparing its predictions to experimental data not used for model identification.

In details, Equation (1) requires knowledge of b_{PCL} and k_{PCL} , the damping and stiffness coefficients of PCL to fully describe the system. To compare and validate the model, data were collected from material testing. A PCL sponge was compressed using a 4.5 kg weight, and images and videos were taken as the PCL reached its maximum deformation. Using this information, Equation (3) can provide approximate k_{PCL} values for the corresponding temperatures.

$$(k_s + k_{PCL}) \cdot \theta_L = T_l = F \cdot L_l. \tag{3}$$

Furthermore, Equation (1) was adjusted to solve for the last unknown b_{PCL} .

$$b_{PCL} = \frac{I_l \ddot{\theta}_L - (k_s + k_{PCL})\theta_L}{\dot{\theta}_I}.$$
 (4)

Once the approximate k_{PCL} values were obtained, the only unknown in Equation (4) is b_{PCL} , then $\dot{\theta}$ and $\ddot{\theta}$ can be calculated from the perturbation data to obtain the values of b_{PCL} at the varying temperatures (Table 1).

In the design of our VIA, the equilibrium position of the compression springs is set at half of the allowed pretension around the central axis (radius = 22.20 mm) (Table 2). Any angular deflection causes the springs to bend and behave in a nonlinear manner as increased forces are applied. As a result, the k_s values used to calculate k_{PCL} (and b_{PCL}) may not be accurate as they are provided by the manufacturer. In addition, the geometry of the PCL fit into each cavity surrounding the central wheel exhibits nonlinear effects on both k_{PCL} and b_{PCL} , as observed during system identification.

The k_{PCL} values follow a clear trend of decreasing magnitude as the temperature increases. Meanwhile, the b_{PCL} values increase as the temperature increases from 30°C to 40°C, before rapidly decreasing as the temperature approaches 60°C. Notably, the b_{PCL} values exhibit a drastic decrease at 55°C, which may be attributed to the nonlinear effects previously observed.

Tracking a trajectory

The motor shaft is commanded in such a way that leads to a sinusoidal trajectory of $A = \pm 20^{\circ}$ amplitude and

Table 1. Viscoelastic Properties of Polycaprolactone

Temperature (°C)	k _{PCL} (N/mm)	b _{PCL} (Ns/mm)
30	52.21	203.54
40	3.38	217.06
50	2.95	70.50
60	2.90	37.88

Table 2. System Parameters

Parameter	Value	
Individual spring stiffness k_s	1.16 N/mm	
Total spring stiffness $12 \cdot k_s$	13.92 N/mm	
Distance of springs from center axis	22.20 mm	
Average distance of PCL from center axis	20.75 mm	
Length of output link L_l	140 mm	
Moment of inertia of output link I_I	$1.20 \times 10^4 \text{ kg} \cdot \text{mm}^2$	
VIA weight	0.86 kg	
Weight attached to output link	0.91 kg	
Maximum angular deflection	±0.2386 rad	
Amount of PCL in each cavity	1.10 g	
Volume of PCL in each cavity	8800 mm ³	

PCL, polycaprolactone; VIA, variable impedance actuator.

 $f = \frac{\omega}{2\pi}$ frequency of 0.5 and 1 Hz for the output link, whereas the PCL temperature is controlled by the flexible heaters. The output link was attached to a rotary encoder, E40S6-2500-3-T-24 from Autonics, with 2500 pulses per revolution (PPR).

Since the output link is not being controlled directly, is compliant, and has both elastic and viscous behavior, we expect to see some amount of overshoot compared with the trajectory of the motor. As the output link becomes more compliance, we should see an increase in the amount of overshoot. In addition, as the output link is in fact a second-order system (*i.e.*, mass-spring damper), we also expect to see some phase delay between the input (*i.e.*, trajectory of the motor) and the output (*i.e.*, trajectory of the output link). Furthermore, these effects should depend on the frequency of the oscillations.

The results are depicted in Figure 6, for two levels of temperature (22°C and 60°C) and two levels of frequency (0.5 and 1 Hz). In each case, the output link started from its stationary position and thus exhibits some irregular transient behavior. However, after a while the output link entered its steady-state case, where it was following a similar sinusoidal trajectory. In each set of experiment, some level of overshooting was noticed.

However, the result showed that when the temperature is high, that is, $\sim 60^{\circ}$ C, the output link trajectory will have greater overshoot, that is, 30% increase from 22°C (blue curve), as the high temperature results in lowering the viscosity of PCL. However, there were no significant differences in the phase delay of the output link encoder values during the trajectory experiments from 22°C to 60°C. This could be due to the fact that both frequencies were small compared with the natural frequency of the output link, and thus the output link is in-phase with the motion of its base (*i.e.*, the motor shaft).

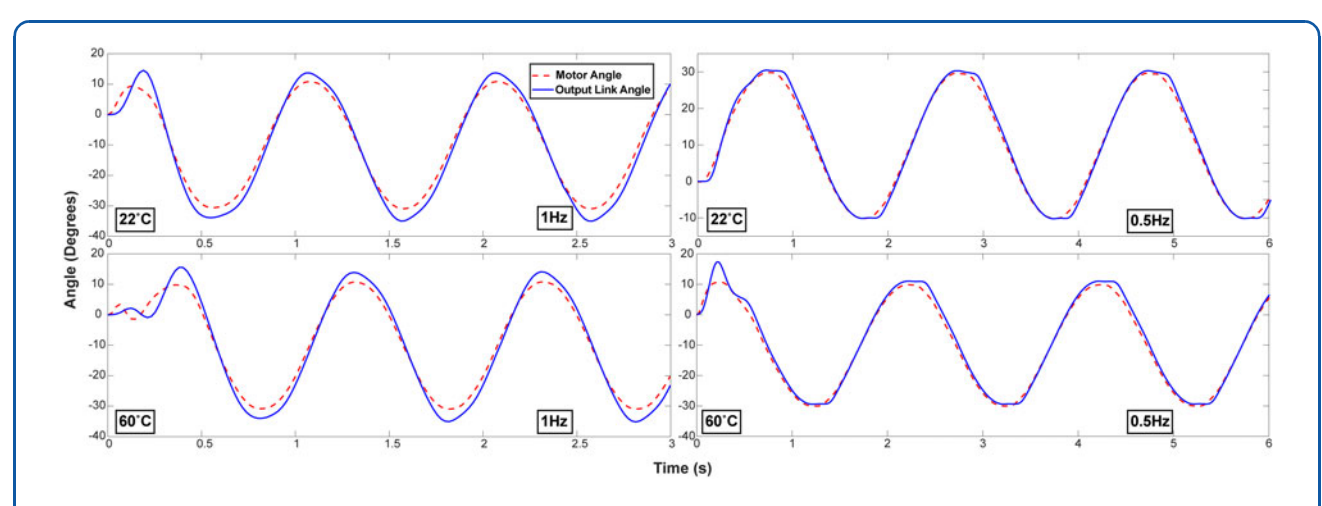


FIG. 6. Following a sinusoidal trajectory for the output link at different temperatures versus expected trajectory.

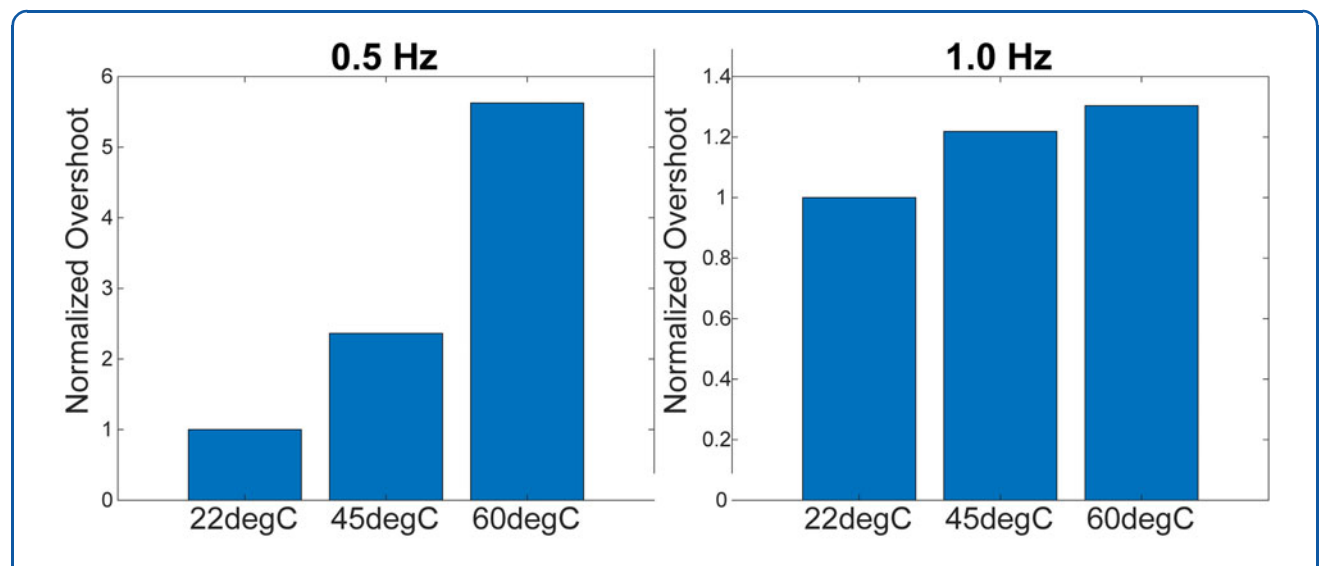


FIG. 7. Overshoot at room (22°C), intermediate (45°C), and high (60°C) temperatures, normalized to room temperature between 0.5 Hz (left) and 1.0 Hz (right) trajectories.

Figure 7 shows the amount of overshoot at three levels of temperature (*i.e.*, 22°C, 45°C, and 60°C) being normalized based on the amount of overshoot at room temperature (*i.e.*, 22°C). As it is clear from the result, at low frequency (*i.e.*, 0.5 Hz), the effect of changing the temperature on the overall impedance of the actuator is very dominant. At 60°C, the amount of overshoot was almost five times of that amount in the room temperature. This clearly shows that our actuator was able to regulate the output impedance by

changing the temperature. However, this effect was less dominant at higher frequency (*i.e.*, 1 Hz), yet still effective. It is important to note that changes in the amount of overshoot are considered as an indicator for impedance regulation, rather than the actual impedance measurement.

Discussion and Conclusion

This article introduces a novel approach to adjusting the impedance of an actuator by regulating the temperature of a viscoelastic polymer, PCL. The temperature control is achieved using flexible polyimide heaters, and a simple design is proposed to enable variable impedance behavior. The lightweight and simplicity of the design can offer new possibilities for developing the next generation of thermoactive VIAs for pHRI applications. The proposed actuator prototype demonstrates the ability to regulate both elasticity and viscosity in an offline manner.

However, the impedance adjustment mechanism is not suitable for online impedance adjustment. Further thermal modeling and optimization are required for online performance. Many actuator systems incorporated into machines have thermal management incorporated. Therefore, identifying active-cooling systems is necessary for online implementation. In addition, we note another limitation of this design that will be improved in future versions, such as the PCL body maintains deformed shapes at room temperature and, therefore, before testing, all heaters were increased >60°C to allow the structure to snap back and fill cavities.

Also, the temperature of the flexible heaters did not accurately represent the total body temperature of PCL, which could be due to air pockets throughout the PCL sponge. The overall rigidity of the PCL bodies was qualitatively examined as temperatures changed. In future study, control systems could be implemented to hold the temperature consistent in the steady state. Additional electrical components may be housed within the body of the housing separate from the heaters to remain isolated from the heat generation.

In future experiments, we aim to optimize the design of our VIA by investigating the packing density and geometry of PCL cavities. Furthermore, since the focus of this study was on offline impedance regulation, the speed of heating was not evaluated, which indicates that further thermal regulation is required for successful implementation. Although the full characterization of temperature-based mechanisms is still an area of active research, a notable advantage is their ability to minimize the overall system footprint by eliminating the need for additional motors.

This compactness makes them particularly valuable for seamless integration into existing setups. We also plan to analyze the effects of scaling down the size of the actuator on the rate of impedance adjustment. In addition, we intend to develop a comprehensive electrothermomechanical model that can be used to analyze the performance of the proposed actuator and

optimize its applicability. Future trajectories should be made more complex in incorporating disturbances/ perturbations, and increasing frequencies to/above the natural frequency of the output link. To improve the transient response, heatsinks can be implemented to make the heat transfer of the module more efficient. Once our VIA is fully realized, we plan to implement it in a small form factor robotic joint for pHRI applications.

Author Disclosure Statement

No competing financial interests exist.

Funding Information

This study was funded by the National Science Foundation NSF under grant number 2045177, and by the National Institute of Health (NIH) through grant number T32GM136501.

References

- 1. Connolly P. Elastic impedance. Leading Edge 199;18(4):438-452.
- Vanderborght B, Albu-Schäffer A, Bicchi A, et al. Variable impedance actuators: A review. Robot Auton Syst 2013;61(12):1601–1614.
- 3. Tonietti G, Schiavi R, Bicchi A. Design and Control of a Variable Stiffness Actuator for Safe and Fast Physical Human/Robot Interaction. In: Proceedings of the 2005 IEEE International Conference on Robotics and Automation. IEEE: Barcelona, Spain; 2005; pp. 526–531.
- Schiavi R, Grioli G, Sen S, et al. Vsa-II: A Novel Prototype of Variable Stiffness Actuator for Safe and Performing Robots Interacting with Humans. In: 2008 IEEE International Conference on Robotics and Automation. IEEE: Pasadena, California; 2008; pp. 2171–2176.
- Jafari A, Tsagarakis NG, Sardellitti I, et al. A new actuator with adjustable stiffness based on a variable ratio lever mechanism. IEEE/ASME Trans Mechatron 2012;19(1):55–63.
- Herr H, Au S, Dilworth P, et al. Artificial Ankle-Foot System with Spring, Variable-Damping, and Series-Elastic Actuator Components, February 22, 2007. US Patent App. 11/495,140.
- Laffranchi M, Tsagarakis NG, Caldwell DG. A Variable Physical Damping Actuator (VPDA) for Compliant Robotic Joints. In: 2010 IEEE International Conference on Robotics and Automation. IEEE: Anchorage, Alaska; 2010; pp. 1668–1674.
- Wagner JT. Variable-Inertia Flywheels and Transmission, May 29, 1990. US Patent 4,928,553.
- Wolf S, Grioli G, Eiberger O, et al. Variable stiffness actuators: Review on design and components. IEEE/ASME Trans Mechatron 2015;21(5): 2418–2430
- Herr H, Paluska D, Dilworth P. Artificial Human Limbs and Joints Employing Actuators, Springs, and Variable-Damper Elements, November 9, 2006. US Patent App. 11/395.448.
- Everarts C, Dehez B, Ronsse R. Novel Infinitely Variable Transmission Allowing Efficient Transmission Ratio Variations at Rest. In: 2015 IEEE/RSJ International Conference on Intelligent Robots and Systems (IROS). IEEE: Hamburg, Germany; 2015; pp. 5844–5849.
- Braun DJ, Howard M, Vijayakumar S. Exploiting Variable Stiffness in Explosive Movement Tasks. In: Robotics: Science and Systems VII. (Newman P, Fox D, Hsu D. eds.) The International Journal of Robotics Research: Berlin, Germany; 2012; p. 25.
- Vanderborght B, Verrelst B, Van Ham R, et al. Exploiting natural dynamics to reduce energy consumption by controlling the compliance of soft actuators. Int J Robot Res 2006;25(4):343–358.
- Nakanishi J, Vijayakumar S. Exploiting Passive Dynamics with Variable Stiffness Actuation in Robot Brachiation. In: Robotics: Science and Systems (Newman P, Fox D, Hsu D. eds.) The International Journal of Robotics Research: Berlin, Germany, Vol. 8; 2013; p. 305.

- Jafari A, Tsagarakis NG, Caldwell DG. Exploiting Natural Dynamics for Energy Minimization Using an Actuator with Adjustable Stiffness (AWAS). In: 2011 IEEE International Conference on Robotics and Automation. IEEE: Shanghai, China; 2011; pp. 4632–4637.
- Morin J-B, Samozino P. Interpreting power-force-velocity profiles for individualized and specific training. Int J Sports Physiol Perform 2016; 11(2):267–272.
- Jafari A. Coupling Between the Output Force and Stiffness in Different Variable Stiffness Actuators. In: Actuators, Vol. 3. (Uchino K. ed.) Multidisciplinary Digital Publishing Institute: Basel, Switzerland; 2014; pp. 270–284.
- Savin S, Golousov S, Khusainov R, et al. Control System Design for Two Link Robot Arm with Maccepa 2.0 Variable Stiffness Actuators. In: 2019 IEEE/ASME International Conference on Advanced Intelligent Mechatronics (AIM). IEEE: Hong Kong, China; 2019; pp. 624–628.
- Jafari A, Quy Vu H, Iida F. Determinants for stiffness adjustment mechanisms. J Intell Robot Syst 2016;82(3–4):435–454.
- Pratt GA, Williamson MM. Series Elastic Actuators. In: Proceedings 1995 IEEE/RSJ International Conference on Intelligent Robots and Systems. Human Robot Interaction and Cooperative Robots, Vol. 1. IEEE: Pittsburgh, Pennsylvania; 1995; pp. 399–406.
- 21. De Santis A, Siciliano B, De Luca A, et al. An atlas of physical human–robot interaction. Mech Mach Theory 2008;43(3):253–270.
- Haddadin S, Albu-Schaffer A, De Luca A, et al. Collision Detection and Reaction: A Contribution to Safe Physical Human-Robot Interaction. In: 2008 IEEE/RSJ International Conference on Intelligent Robots and Systems. IEEE: Nice, France; 2008; pp. 3356–3363.
- Colgate E, Bicchi A, Aaron Peshkin M, et al. Safety for Physical Human-Robot Interaction. In: Springer Handbook of Robotics. (Siciliano B, Khatib O. eds.) Springer: Berlin, Germany; 2008; pp. 1335–1348.
- Tsagarakis NG, Laffranchi M, Vanderborght B, et al. A Compact Soft Actuator Unit for Small Scale Human Friendly Robots. In: 2009 IEEE International Conference on Robotics and Automation. IEEE: Kobe, Japan; 2009; pp. 4356–4362.
- Robinson DW, Pratt JE, Paluska DJ, et al. Series Elastic Actuator Development for a Biomimetic Walking Robot. In: 1999 IEEE/ASME International Conference on Advanced Intelligent Mechatronics (Cat. No. 99TH8399). IEEE: Atlanta, Georgia; 1999; pp. 561–568.
- Sergi F, Accoto D, Carpino G, et al. Design and Characterization of a Compact Rotary Series Elastic Actuator for Knee Assistance During Overground Walking. In: 2012 4th IEEE RAS & EMBS International Conference on Biomedical Robotics and Biomechatronics (BioRob). IEEE: Roma, Italy; 2012; pp. 1931–1936.
- Grimmer M, Eslamy M, Gliech S, et al. A Comparison of Parallel-and Series Elastic Elements in an Actuator for Mimicking Human Ankle Joint in Walking and Running. In: 2012 IEEE International Conference on Robotics and Automation. IEEE: St. Paul, Minnesota; 2012; pp. 2463–2470.
- Campbell E, Chad Kong Z, Hered W, et al. Design of a Low-Cost Series Elastic Actuator for Multi-Robot Manipulation. In: 2011 IEEE International Conference on Robotics and Automation. IEEE: Shanghai, China; 2011; pp. 5395–5400.
- Aukes D, Kim S, Garcia P, et al. Selectively Compliant Underactuated Hand for Mobile Manipulation. In: 2012 IEEE International Conference on Robotics and Automation. IEEE: St. Paul, Minnesota; 2012; pp. 2824–2829.
- Suarez A, Heredia G, Ollero A. Lightweight Compliant Arm for Aerial Manipulation. In: 2015 IEEE/RSJ International Conference on Intelligent Robots and Systems (IROS). IEEE: Hamburg, Germany; 2015; pp. 1627–1632.
- 31. Manfredi L, Huan Y, Cuschieri A. Low power consumption mini rotary actuator with SMA wires. Smart Mater Struct 2017;26(11):115003.
- 32. San-Miguel A, Alenyà G, Puig V. Automated off-line generation of stable variable impedance controllers according to performance specifications. IEEE Robot Autom Lett 2022;7(3):5874–5881.
- Walker DS, Salisbury JK, Niemeyer G. Demonstrating the Benefits of Variable Impedance to Telerobotic Task Execution. In: 2011 IEEE International Conference on Robotics and Automation. IEEE: Shanghai, China; 2011; pp. 1348–1353.

- Labet M, Thielemans W. Synthesis of polycaprolactone: A review. Chem Soc Rev 2009;38(12):3484–3504.
- Briand D, Colin S, Gangadharaiah A, et al. Micro-hotplates on polyimide for sensors and actuators. Sens Actuators A Phys 2006;132(1):317–324.
- 36. Liu J, Liu L. Ring-opening polymerization of ε-caprolactone initiated by natural amino acids. Macromolecules 2004;37(8):2674–2676.
- 37. Yu T-L, Wu C-C, Chen C-C, et al. Catalysts for the ring-opening polymerization of ε -caprolactone and l-lactide and the mechanistic study. Polymer 2005;46(16):5909–5917.
- 38. Kimmich R, Fatkullin N. Polymer Chain Dynamics—Chapter 3: Polymer Viscoelasticity. In: NMR• 3D Analysis• Photopolymerization. (Fatkullin N. ed.) Springer: Berlin, Germany; 2004; pp. 1–113.
- Watanabe H. Viscoelasticity and dynamics of entangled polymers. Progr Polym Sci 1999;24(9):1253–1403.
- Aradian Á, Raphael E, De Gennes P-G. Strengthening of a polymer interface: Interdiffusion and cross-linking. Macromolecules 2000;33(25): 9444–9451.
- 41. Ulanski P, Bothe E, Hildenbrand K, et al. Free-radical-induced chain breakage and depolymerization of poly (methacrylic acid): Equilibrium polymerization in aqueous solution at room temperature. Chemistry 2000;6(21):3922–3934.
- 42. Vanapalli SA, Ceccio SL, Solomon MJ. Universal scaling for polymer chain scission in turbulence. Proc Natl Acad Sci 2006;103(45):16660–
- 43. Stone A. The Theory of Intermolecular Forces. Oxford University Press: Cambridge, England; 2013.
- Exley T, Johnson D, Jafari A. Towards a novel thermal-based variable impedance module through adjusting viscoelastic properties of a thermoresponsive polymer. IEEE Trans Med Robot Bionics 2023;5(4):1110– 1113.
- Mosleh Y, Ebrahimi NG, Mahdavian A, et al. TPU/PCL/nanomagnetite ternary shape memory composites: Studies on their thermal, dynamicmechanical, rheological and electrical properties. Iran Polym J 2013;23(2):137–145.
- Johnson AR, Quigley CJ. A viscohyperelastic maxwell model for rubber viscoelasticity. Rubber Chem Technol 1992;65(1):137–153.
- Hosford WF. Mechanical Behavior of Materials. Cambridge University Press: Cambridge, England; 2010.
- Vizesi F, Jones C, Lotz N, et al. Stress relaxation and creep: Viscoelastic properties of common suture materials used for flexor tendon repair. J Hand Surg 2008;33(2):241–246.
- 49. Rivlin RS. The elasticity of rubber. Rubber Chem Technol 1992;65(3): 51–66.

Cite this article as: Exley T, Johnson D, Jafari A (2023) A novel variable impedance actuator utilizing adjustable viscoelastic properties of thermoresponsive *polycaprolactone*. *Robotics Reports* 1:1, 57–66, DOI: 10.1089/rorep.2023.0017.

Abbreviations Used

 $\mathsf{HRI} = \mathsf{human}\text{--}\mathsf{robot} \; \mathsf{interaction}$

PCL = polycaprolactone

PETG = polyethylene terephthalate glycol pHRls = physical human-robot interactions

SEA = series elastic actuator

VIA = variable impedance actuator

VSA = variable stiffness actuator